EXTERIOR BEAM-COLUMN JOINTS IN REINFORCED CONCRETE FRAMES

M. Seckin[I] and S.M. Uzumeri[II]

SUMMARY

Nine full size beam-column sub-assemblies have been tested at the University of Toronto. The columns were subjected to varying levels of axial compression while the beams were subjected to full inelastic moment reversals in both directions.

The paper briefly summarizes the results of the experimental program. In addition, hysteretic behaviour of beam and its energy dissipation characteristics are computed based on the measured stress versus strain characteristics of the steel and concrete, and are compared to the experimentally determined properties of the sub-assembly.

EXPERIMENTAL RESULTS

The experimental program carried out at the University of Toronto to date involved the testing of nine specimens, simulating an exterior sub-assembly, under slow load reversals. The geometrical and material properties of these specimens and the test results are given elsewhere [1,2,3]. The test specimens SP1-SP4 had 305 mm x 510 mm, and SP5-SP9 had 380 mm x 510 mm beams framing into 380 mm x 380 mm columns. The column height and beam length measured from the column centreline were 3050 mm. The columns of the specimens were subjected to varying levels of axial compression from $0.09P_o$ to $0.79P_o$, while the beams were subjected to full inelastic reversals in both directions. To determine the strain distribution along the reinforcement, beam and column steel were instrumented with electrical strain gauges. Following is a brief summary of conclusions of the experimental program [1,2,3].

1. Stirrups are essential at the beam-column joints of reinforced concrete frames in seismic risk areas, to provide confinement and shear resistance to the joint and to increase the ability of the joint to provide continued anchorage to beam steel. Stirrups to be effective must be fully anchored in the core.

2. The assumption of rigid beam-column connections utilized in inelastic dynamic analysis of reinforced concrete frame structures may give invalid results.

3. Ductility in the joint is undesirable. The primary aim of the designer should be to prevent the yielding of the joint steel. Steel with a stress vs strain characteristic that exhibits a flat yield plateau may be undesirable as joint confinement steel.

I Graduate Student, Department of Civil Engineering, University of Toronto, Toronto, Ontario, Canada

II Professor, Department of Civil Engineering, University of Toronto, Toronto, Ontario, Canada

4. The quality of anchorage provided by the joint to the beam has a very significant effect on the energy dissipation characteristics of the beam. When the beam steel is subjected to reversed plasticity, there is a gradual deterioration of bond between concrete and steel and at some stage, the entire force in the bar is transferred to, and resisted by the hook. In addition, proper distribution of the column steel around the perimeter of the joint improves the behaviour of the sub-assembly. The contribution of distributed steel to shear strength as well as to the effective confinement of the concrete core are significant.

5. In the case of one specimen (SP8), the fulfilment of the current code requirements was not adequate to ensure the formation of the plastic hinge in the beam rather than in the column. Hinging of the column due to the cover spalling results in an unsatisfactory behaviour; therefore the computation of the ultimate flexural strengths of the column at the design axial load should be based on the strength of the core and the contribution of the cover should be disregarded.

6. The magnitude of column axial compressive force had little effect on the behaviour of a well designed exterior joint.

The lack of agreement among various researchers on the definition of physical properties (i.e., yield deflection, ductility factor, etc.) and the use of these terms without a clear definition make meaningful comparison of various test results very difficult. There is no agreement, as yet, as to how a well designed joint should perform. Furthermore, the observed performance is clearly dependent on the loading sequence and loading levels utilized. Therefore the development of a set of "realistic expectations of performance" for joints based on the required ductility of adjoining beams would be the most important step towards the formulation of rational design procedures for the joints. This is a particularly important topic because the results obtained from the tests in which the joints have been subjected to unrealistically severe loading may result in unnecessarily severe design rules, with the accompanying difficulty of construction and the increased costs.

Development of realistic performance criteria and loading regimes must relate to the demand of the earthquake upon the structure. Therefore, there is a need to develope realistic mathematical behavioural models for use in determination of the response of a structure.

ANALYTICAL MODEL

Comparison of the behaviour of various beam-column sub-assemblies is based on the beam tip load versus beam tip deflection characteristics of the specimens.

The following factors contribute to the deflection of the beam tip: a) Deflection due to flexural deformation of the beam, b) Deflection due to the shear deformation of the beam, c) Deflection due to the deformation of the column, and d) Deflection due to deformation originating from the beam-column joint panel zone. In the specimens tested in this research, the contribution of the shear deformation of the beam to the beam tip deflection was negligible [2]. In addition, in these specimens, the column essentially

remained in the linear range, and the contribution of column deformation to the beam tip deflection could be deduced readily.

To model the effect of the remaining two factors, mathematical models for concrete and steel are developed, and the beam tip deflection is computed. These tip deflections are compared with the experimental deflection due to flexure only. Subsequently, the contribution of the joint deformation is considered and the calculated and observed behaviour of the sub-assembly is compared.

Modelling of Concrete Behaviour

Forty-eight unconfined 152 mm x 305 mm (6inx12in) concrete cylinders were tested under several repeated loading programs. The concrete strength of the specimens varied from 24.1 MPa (3500 psi) to 41.4 MPa (6000 psi). In these tests, test speed was kept constant at the rate of 0.4 mm/min (0.016 in/min).

Fig. 1(a) shows the analytical model, which consists of three segments representing the stress vs strain curve. An exponential expression (Eq.1) which is a function of concrete strength is used to predict the stress-strain curve of the concrete under monotonic compression. This curve is also the envelope curve for specimens subjected to repeated loading. Unloading (Eq.2) and reloading (Eq.3) curves are represented by degrading functions. Tensile strength of concrete is disregarded.

An application of the analytical model to one of the test specimens is shown in Fig. 2. For all thirty specimens tested, the predicted and observed hysteresis curves were in close agreement.

Modelling of Reinforcing Steel Behaviour

The analytical model to predict the behaviour of steel is given in Fig. 1(b). The parameters of the Equations (4), (5) and (6) were empirically determined from twenty-five coupon tests on #8-#10 bars (25mm-32mmØ). In the modelling, an attempt is made to include both the strain hardening effect and the Bauschinger Effect.

Tests under monotonic loading yielded the tri-linear stress-strain curve (Eq.4). Presence of previous plastic strains will affect the unloading and reloading curves according to the strain history. (Eq.5) is a degrading straight line approximation to the unloading curves. Bauschinger Effect is represented by (Eq.6). In this equation the constants of the expression are obtained by considering the origin and end point of the curve.

Figures 3 and 4 show a comparison of calculated and experimentally determined stress-strain curves of steel both in tensile and compressive regions.

Modelling of the Beam Behaviour

A computer program was developed to obtain the moment-curvature relationship of reinforced concrete cross-sections, utilizing the concrete

and steel models referred to above. For computation of the tip deflection, the beam of the sub-assembly was divided into eleven 254 mm (10 in) long segments. Beams of the test sub-assemblies of three specimens were similarly divided into eleven segments and the rotation of each segment was measured. From these measured rotations, the tip deflection due to flexure was calculated [2].

Modelling of Exterior Joint Core Behaviour

The contribution of the joint core deformation to the beam tip deflection is considered in two parts. Beam bars anchored in the exterior joint consists of two segments, namely the straight lead embedment and the bend, Fig. 5(a). The tensile force in the beam bars are resisted initially by bond along the lead embedment. However, the bond is lost in early stages of loading [3] and in the latter stages of loading most of the resistance is offered by the compressive strut under the bend. The contribution of the lead embedment deformation to the tip deflection is computed by considering that in the latter stages of loading history, the strain in the lead embedment segment is uniform.

As a result of the tendency of the bend to press down on the concrete, the bar will assume the new position shown in Fig. 5(b). Free body diagram of a segment of the bar at the bend is given in Fig. 5(c).

The contribution of the bend deformation to the tip deflection of the beam is calculated from the horizontal displacement Δ_{BX} of the starting point of the bend. At any stage of loading the magnitude of Δ_{BX} is obtained through iterations to balance the forces acting on the bar. The following assumptions were made in the iterative process:

1. For the loading stage considered, the bars only with tensile stresses are considered to press on the diagonal struts. The compression bars are assumed to return to their original undeformed position.

2. Resistance to the tensile force, T_{hook}, acting at the start of the bend, is supplied by the forces F_i, created on the struts and the friction force F_{fi}, between the bar surface and the concrete as shown in Fig. 5(c).

3. The deformations are such that the original shape of the bend does not change when it assumes the new position. Thus, as shown in Fig. 5(b), the displacement of the bar is taken to be due only to the rotation of the bend about the tail end.

In the iterative procedure the bend and the tail are divided into ten segments. It is assumed that the inclination of the compression struts are at 45 degrees. A value for Δ_{BX} is assumed. The displacement of each of the segments are computed in terms of assumed Δ_{BX}. From these calculated deformations, the diagonal compression force F_i and the friction force F_{fi} are computed. In calculating F_i, the area and length of each strut is considered. The stress-strain curve for the confined concrete in the core was based on Sheikh-Uzumeri model [4]. The coefficient of friction was taken as 0.3. The sum of the horizontal components of the forces acting on each of the ten segments are compared with the tension force at the begining

of the bend, T_{hook}. Then the value of Δ_{BX} is adjusted until the sum of the horizontal forces are in equilibrium.

The results of the analytical study are summarized in Fig. 6.. The factors contributing to the beam-tip deflection are illustrated in Fig. 6(a). Fig. 6(b) shows the comparison of calculated and experimentally observed beam tip deflection hysteresis loops for specimen SP7. In this comparison, only the contribution of beam flexure is taken into account. Beam tip deflection hysteresis loops due to the column response is shown in Fig. 6(c). Additional contributions of the two types of joint deformation, deformation in the lead length and deformation due to bend movement are shown in Fig. 6(d) and 6(e), respectively. Fig. 6(f) shows the calculated beam tip deflection curves for the sub-assembly, taking into account the contribution of all of the factors. In addition, in Fig. 6(f), the experimentally observed hysteresis loops are plotted for comparison purposes. Figures 6(g) and 6(h) show the relationship between the computed and the observed absolute cumulative beam tip deflection and the energy input.

CONCLUSIONS

Conclusions from the experimental work are summarized at the beginning of the paper. Analytical model, which is still under development, appears to predict the experimental behaviour of the specimens. It appears that when the response characteristics of the sub-assembly are to be modelled, the contribution of the joint region should not be neglected.

ACKNOWLEDGEMENTS

Research reported is supported by a Natural Sciences and Engineering Research Council of Canada Grant (NSERC A4273) and by the University of Toronto. Experimental work was conducted in the Structures Laboratory of the Department of Civil Engineering of the University of Toronto.

REFERENCES

[1] Uzumeri, S.M., and Seckin, M., "Behaviour of Joints and Ductility of Reinforced Concrete Frames", Proceedings of the Fifth European Conference on Earthquake Engineering, Istanbul, Turkey, September 1975, Vol. 2, Paper No. 94, 14pp.

[2] Uzumeri, S.M., "Strength and Ductility of Cast-in-Place Beam-Column Joints", Reinforced Concrete Structures in Seismic Zones, Publication SP-53, American Concrete Institute, pp. 293-350, Detroit, 1977.

[3] Seckin, M., and Uzumeri, S.M., "Examination of Design Criteria for Beam-Column Joints", Proceedings of the Sixth European Conference on Earthquake Engineering, Dubrovnik, Yugoslavia, September 1978, Vol. 3, pp 175-182.

[4] Sheikh, S.A., and Uzumeri, S.M., "Properties of Concrete Confined by Rectangular Ties", Proceedings of A.I.C.A.P - C.E.B Symposium on Structural Concrete Under Seismic Actions, Rome, Italy, May 1979, CEB Bulletin D'information No.132, pp 53-60.

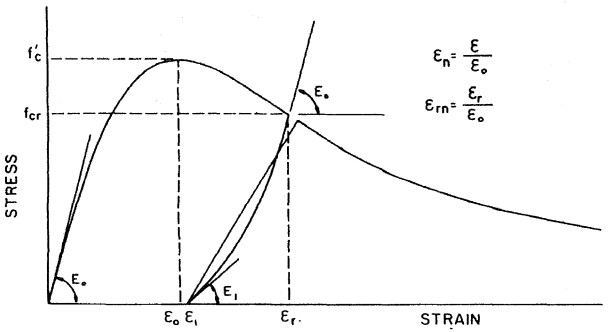

(a) Model for Concrete

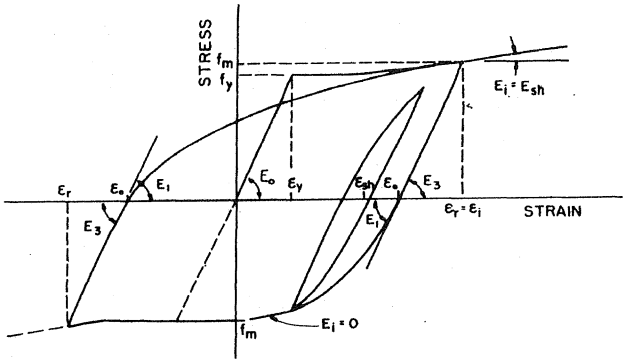

(b) Model for Reinforcing Steel

ENVELOPE CURVE $$f_c = \frac{f'_c}{1+B}\,\varepsilon_n^C\, e^{C(1-\varepsilon_n^A)/A} + B - \frac{B}{e^{5\varepsilon_n}} \quad \text{...eq.(1)}$$

UNLOADING CURVE $$f_c = E_1(\varepsilon-\varepsilon_1) + D\,(\varepsilon-\varepsilon_1)^N \quad \text{...eq.(2)}$$

RELOADING CURVE $$f_c = \frac{8.1\,E_o}{\varepsilon_1 E_o + 73.5}(\varepsilon-\varepsilon_1) \quad \text{...eq.(3)}$$

PARAMETERS

$$A = 0.074\,f'_c - 1.21 = 1.85$$

$$B = -0.013\,f'_c + 0.89 = 0.35$$

$$C = -0.022\,f'_c + 2.65 = 1.75$$

$$D = (f_{cr} - E_1\varepsilon_1)\,/\,\varepsilon_1^N$$

$$E_1 = \begin{cases} E_o\,(1 - 0.7\,\varepsilon_{rn}^{0.41}) & \text{if } \varepsilon_r < 2\varepsilon_o \\ 0.071\,E_o & \text{if } \varepsilon_r \geq 2\varepsilon_o \end{cases}$$

$$\varepsilon_1 = \begin{cases} 0.335\,\varepsilon_o\,(\varepsilon_{rn})^{2.06} & \text{if } \varepsilon_r < 2\varepsilon_o \\ \varepsilon_r - 0.75\,\varepsilon_o & \text{if } \varepsilon_r \geq 2\varepsilon_o \end{cases}$$

$$N = \frac{(E_o - E_1)(\varepsilon_r - \varepsilon_1)}{f_{cr} - E_1(\varepsilon_r - \varepsilon_1)}$$

FIRST LOADING

(a) $f(\varepsilon) = E\varepsilon \qquad \varepsilon \leq \varepsilon_y$

(b) $f(\varepsilon) = f_y \qquad \varepsilon_y \leq \varepsilon \leq \varepsilon_{sh}$

(c) $f(\varepsilon) = f_y + (\varepsilon - \varepsilon_{sh})\,E_{sh} \qquad \varepsilon_{sh} < \varepsilon$ ...eq.(4)

UNLOADING CURVES $$f(\varepsilon) = f_m - E_3(\varepsilon - \varepsilon_r) \quad \text{...eq.(5)}$$

RELOADING CURVES $$f(\varepsilon) = E_1(\varepsilon - \varepsilon_o) + \frac{E_i - E_1}{n(\varepsilon_i - \varepsilon_o)^{n-1}}(\varepsilon - \varepsilon_o)^n \quad \text{...eq.(6)}$$

PARAMETERS

$$E_1 = E\,(0.98 - 0.083\,\frac{\varepsilon_r - \varepsilon_o}{\varepsilon_y})$$

$$E_3 = \begin{cases} E_o & (\varepsilon_r - \varepsilon_o) \leq \varepsilon_y \\ \frac{E_o}{20}\,(21 - \frac{\varepsilon_r}{\varepsilon_y}) & \varepsilon_y < (\varepsilon_r - \varepsilon_o) < 4\varepsilon_y \\ 0.85\,E_o & 4\varepsilon_y \leq (\varepsilon_r - \varepsilon_o) \end{cases}$$

$$n = \frac{(E_i - E_1)(\varepsilon_i - \varepsilon_o)}{f_i - E_1(\varepsilon_i - \varepsilon_o)}$$

Fig. 1. Stress-strain Curve Models for Concrete and Reinforcing Steel

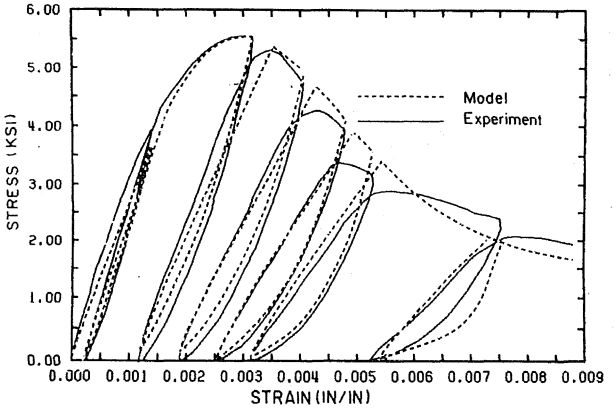

Fig. 2. Stress-strain Behaviour of Concrete with Cyclic Loading

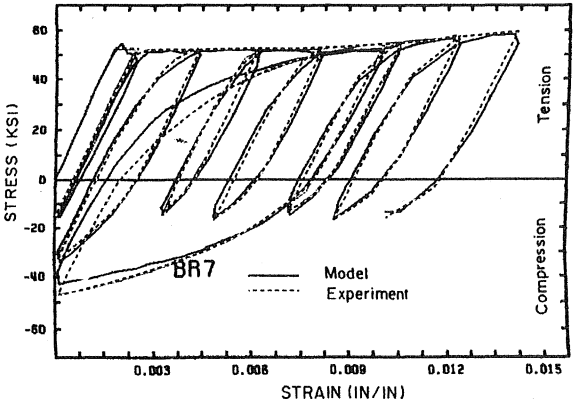

Fig. 3. Stress-strain Behaviour of Reinforcing Steel with Reversed Loading (Tension)

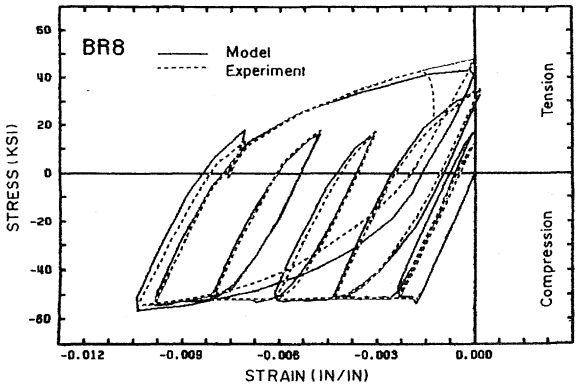

Fig. 4. Stress-strain Behaviour of Reinforcing Steel with Reversed Loading (Compression)

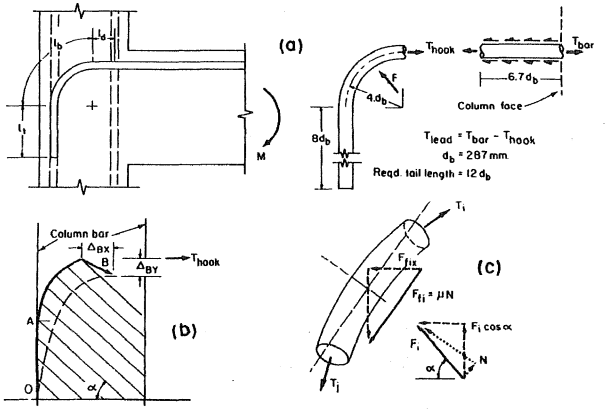

Fig. 5. Development of Model for Exterior Joint Core

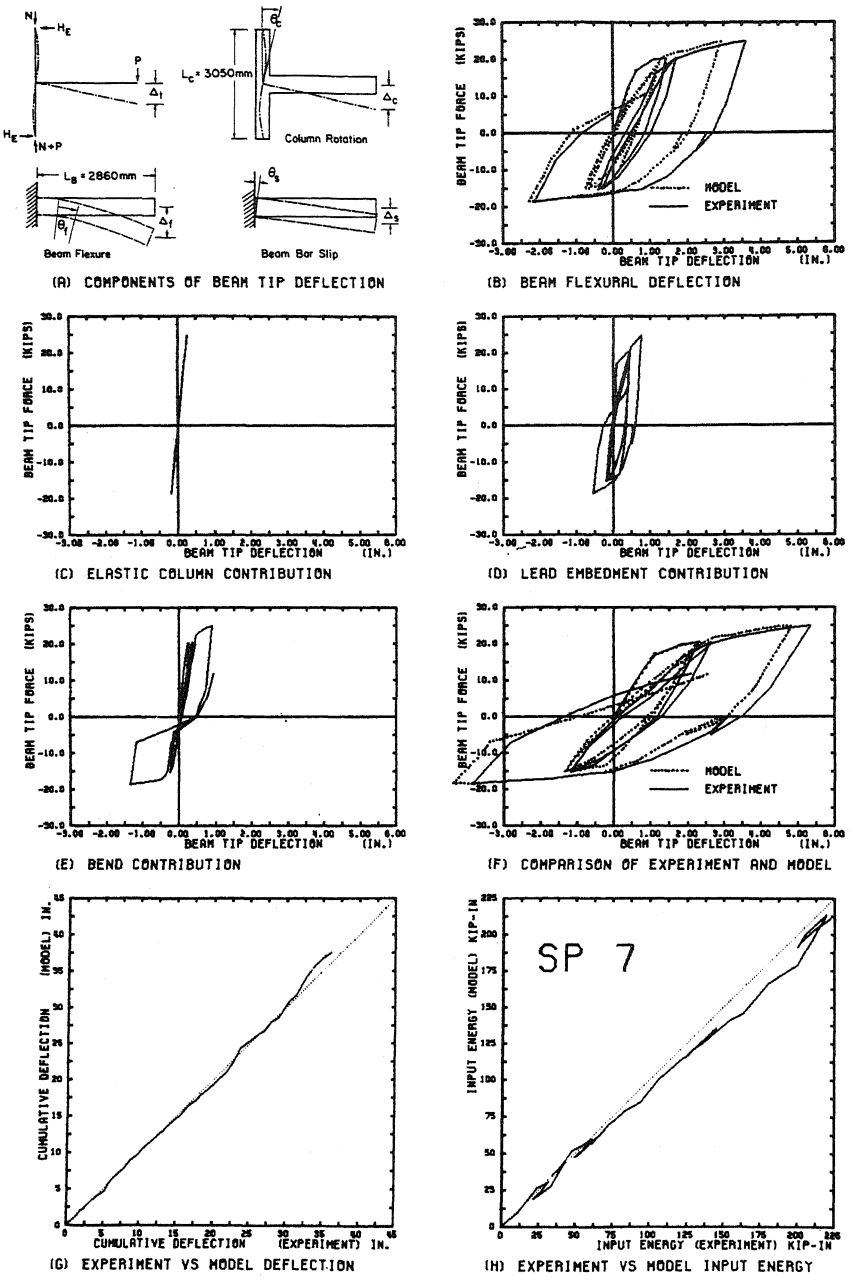

Fig. 6. Comparison of Measured and Computed Beam Tip Load vs. Deflection Curves for SP7